

Cover Page



Universiteit Leiden

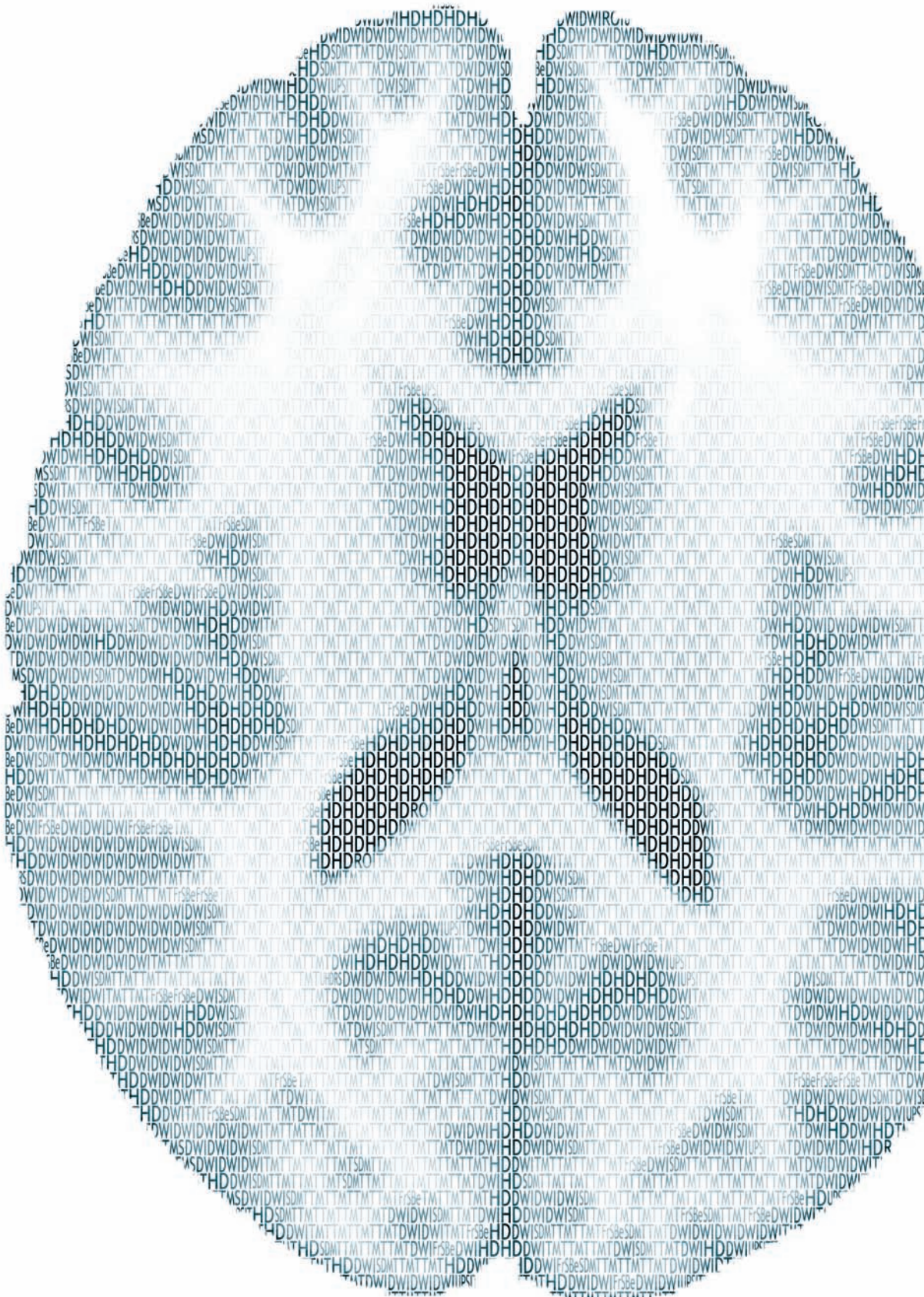


The handle <http://hdl.handle.net/1887/20120> holds various files of this Leiden University dissertation.

Author: Bogaard, Simon Johannes Adrianus van den

Title: Huntington's disease : quantifying structural brain changes

Date: 2012-11-14





CHAPTER 6

EARLY CHANGES IN WHITE MATTER PATHWAYS OF THE SENSORIMOTOR CORTEX IN PREMANIFEST HUNTINGTON'S DISEASE

EVE M. DUMAS¹, SIMON J.A. VAN DEN BOGAARD¹, MARGOT E. RUBER¹,
RALF REILMANN², JULIE C. STOUT^{3,4}, DAVID CRAUFURD⁵,
STEPHEN L. HICKS⁶, CHRIS KENNARD⁶,
SARAH J. TABRIZI⁷, MARK A. VAN BUCHEM⁸,
JEROEN VAN DER GROND⁸, AND RAYMUND A.C. ROOS¹

1. DEPARTMENT OF NEUROLOGY, LEIDEN UNIVERSITY MEDICAL CENTRE, LEIDEN, THE NETHERLANDS

2. DEPARTMENT OF NEUROLOGY, UNIVERSITY OF MUNSTER, MUNSTER, GERMANY

3. SCHOOL OF PSYCHOLOGY, PSYCHIATRY AND PSYCHOLOGICAL MEDICINE, MONASH UNIVERSITY,

CLAYTON CAMPUS, VIC, AUSTRALIA

4. DEPARTMENT OF PSYCHOLOGICAL AND BRAIN SCIENCES, INDIANA UNIVERSITY, BLOOMINGTON, INDIANA, USA

5. GENETIC MEDICINE, UNIVERSITY OF MANCHESTER, MANCHESTER ACADEMIC HEALTH SCIENCES CENTRE,

MANCHESTER, UNITED KINGDOM

6. CENTRAL MANCHESTER UNIVERSITY HOSPITALS NHS FOUNDATION TRUST, ST. MARY'S HOSPITAL, MANCHESTER,

UNITED KINGDOM

7. DEPARTMENT OF CLINICAL NEUROLOGY, UNIVERSITY OF OXFORD, UNITED KINGDOM, UCL INSTITUTE OF

NEUROLOGY, UNIVERSITY COLLEGE LONDON, QUEEN SQUARE, LONDON, UNITED KINGDOM

8. DEPARTMENT OF RADIOLOGY, LEIDEN UNIVERSITY MEDICAL CENTRE, LEIDEN, THE NETHERLANDS

Abstract

Objectives

To investigate the function-structure relationship of white matter within different stages of Huntington's disease using diffusion tensor imaging (DTI).

Experimental design

From the TRACK-HD study, an early stage HD group and a pre-manifest gene carrier group (PMGC) were age-matched to two healthy control groups; all underwent 3T MRI scanning of the brain. Region of interest (ROI) segmentation of the corpus callosum, caudate nucleus, thalamus, prefrontal cortex and sensorimotor cortex was applied, and the apparent fiber pathways of these regions were analyzed. Functional measures of motor, oculomotor, cognition, and behavior were correlated to DTI measures.

Principle observations

In PMGC versus controls, higher apparent diffusion coefficient (ADC) was seen in white matter pathways of the sensorimotor cortex ($p < 0.01$) and in the ROI of corpus callosum ($p < 0.017$). In early HD, fiber tract analysis showed higher ADC in pathways of the corpus callosum, thalamus, sensorimotor and pre-frontal region ($p < 0.01$). ROI analysis showed higher diffusivity in the corpus callosum and caudate nucleus ($p < 0.017$). Motor, oculomotor, cognition, and probability of onset within 2 and 5 years, correlated well with ADC measures of the corpus callosum ($p < 0.01 - p < 0.005$), sensorimotor ($p < 0.01 - p < 0.005$) and prefrontal region ($p < 0.01$).

Conclusions

Disturbances in the white matter connections of the sensorimotor cortex can be demonstrated not only in manifest HD but also in pre-manifest gene carriers. Connectivity measures are well related to clinical functioning. DTI measures can be regarded as a potential biomarker for HD, due to their ability to objectify changes in brain structures and their role within brain networks.

Introduction

Huntington's disease (HD) is a neurodegenerative genetic disorder characterized by a progressive deterioration of motor control, cognitive functioning, and mood and behavioral functioning. The presence of an abnormal expansion of CAG repeats in the *HTT* gene, on chromosome four is responsible for the disease. The effect of the HD gene is seen in the brain as progressive cerebral atrophy of the basal ganglia and cortex¹⁻⁴. It has been shown that the onset of atrophy may already be present in gene carriers up to 10 years prior to disease manifestation^{4,5}. On the contrary, less is known about white matter changes in HD. Some reports demonstrate global atrophy of the white matter in manifest HD^{6,7}, whereas others show regional differences only^{8,9}. A global volume reduction of white matter was seen only in one study of premanifest gene carriers¹⁰. The specific impact of HD on specific white matter pathways, and the clinical relevance of these changes, remains unclear.

The development and clinical application of magnetic resonance diffusion tensor imaging (DTI) has increased knowledge of grey and white matter structure in a variety of neurodegenerative diseases¹¹. In patients with HD, a few studies have applied DTI to characterize changes in the macrostructure and microstructure of the basal ganglia. Lower fractional anisotropy (FA) values were found for premanifest gene carriers in the putamen, caudate nucleus¹² and thalamus³. On the contrary, Rosas *et al.* (2006) found higher FA in the putamen and pallidum¹⁴. In healthy subjects, FA values of grey matter structures are generally below 0.15. In white matter, values tend to be much higher ranging from 0.2 up to 1¹⁵. In general, the higher the FA value the more directional the organization of the tissue is regarded to be - as seen in white matter fiber tracts. For this reason FA is generally accepted as an indication of tissue integrity.

In white matter, lower FA and increased apparent diffusion coefficient (ADC) values have been found in the internal capsule and corpus callosum in premanifest and manifest HD compared with healthy control subjects^{13,14}. In several of neurodegenerative disorders, such as Alzheimer's and Parkinson's Disease, ADC values have been found to higher, indicating that degeneration negatively affects the brain tissue structure¹⁶⁻¹⁸. Higher ADC values indicate that the microstructure of the tissue allows a faster movement of water molecules. These higher values were also found in manifest HD¹⁹⁻²². To find white matter differences that are related to the earliest changes in HD, specific white matter fiber tracts that are related to HD symptomatology should preferably be investigated. A reduction in cognitive, motor,

oculomotor performance is present up to a decade before clinical manifestation of HD^{5,23,24}, therefore, it can be hypothesized that the fibers associated with these function may also be affected in the premanifest phase. The direct nature of this relationship is unknown, and therefore, the aim of the present study is, first, to investigate early FA and ADC changes in white matter fiber bundles running to and from brain areas known to be affected by HD (e.g. caudate nucleus) or those related to the clinical characteristics of HD (e.g. sensorimotor cortex or prefrontal cortex). Second, to investigate to which extent changes in brain tissue structure and integrity in white matter fibers are related to clinical functioning.

Method

Participants

As part of the Track-HD study 90 participants were included at the Leiden University Medical Centre study site (for details see Tabrizi *et al.*, 2009⁴). Diffusion tensor magnetic resonance imaging was added to the standard MRI protocol. DTI was not performed because of claustrophobia in 10 participants, and another nine were excluded from analysis due to movement artifacts. Of the remaining 71 subjects, 16 subjects had early HD, 27 were premanifest gene carriers and 28 were healthy control subjects. Inclusion criteria for premanifest HD gene carriers were a CAG repeat ≥ 40 with a total motor score on the Unified Huntington's Disease Rating Scale 1999 (UHDRS) ≤ 5 . Inclusion criteria for the early manifest HD patients were a CAG repeat ≥ 40 , with a UHDRS motor score > 5 and a total functional capacity (TFC) score ≥ 7 . Healthy gene negative family members or partners were recruited as control subjects. Because the early HD group is inherently older than the premanifest group, the control group was split into two separate groups of each 14 subjects to achieve age-matching. The younger healthy control subjects were age matched to the premanifest gene carriers (control group A). The older healthy controls subjects were age-matched to the manifest group (control group B). None of the participants suffered from a neurological disorder, a major psychiatric diagnosis, or had a history of severe head injury. The study was approved by the Medical Ethical Committee of the Leiden University Medical Centre. All participants gave informed consent.

DTI acquisition

MRI acquisition was performed on a 3 Tesla whole body scanner (Philips Achieva, Healthcare, Best, the Netherlands) with an eight channel SENSE head coil. T1-weighted image volumes were acquired using a 3D MPRAGE acquisition sequence with the following imaging parameters: TR = 7.7 ms, TE = 3.5 ms,

FOV = 24 cm, matrix size 224x224, number of slices = 164, slice thickness = 1.00 mm, slice gap = 0. A volumetric T2-weighted image (VISTA) was acquired with the same parameters for field of view, acquisition matrix, and slice thickness as the T1-weighted images, with TE = 250 ms and TR = 2500 ms. A single-shot echo-planar DTI sequence was applied with 32 measurement directions and the following scan parameters: TR = 10004 ms, TE = 56 ms, FOV = 220 x 220 x 128 with an acquisition matrix of 112 x 110, 2.00 mm slice thickness, transversal slice orientation, slice gap = 0, flip angle = 90°, single reconstruction voxel dimensions were 1.96 x 1.96 x 2.00 mm, number of slices = 64, B factor = 1000, halfscan factor = 0.61. Parallel imaging (SENSE) was used with a reduction factor of 2, NSA = 1 and fat suppression was applied. DTI acquisition time was 6.55 minutes.

Regions of interest segmentation

A priori, the caudate nuclei, thalami, and the corpus callosum were determined as regions of interest (ROI). A semiautomatic segmentation and analysis procedure was used as part of the software program FibreTrak (release 2.5.3, Philips Medical Systems, Best, the Netherlands). The caudate nucleus and thalamus were segmented separately on each side, but considered as one ROI during data analysis. On the DTI scans, special caution was taken to prevent inclusion of any non grey matter voxels, as both the caudate nucleus and thalamus are laterally bordered by the internal capsule. All analyses and segmentations were performed blinded to group status. For more detailed information on segmentations see the supplementary material.

Fiber tract analysis

Fiber analysis of fibers running through the following five structures was performed: the corpus callosum (Figure 1A), sensorimotor cortex (Figure 1B), caudate nucleus (Figure 1C), superior prefrontal cortex (Figure 1D) and thalamus (Figure 1E). To analyze fibers running through the corpus callosum, caudate nucleus and thalamus, the previously segmented ROIs were used. Additional segmentations for ROIs of the superior prefrontal cortex and sensorimotor cortex were performed. The superior prefrontal region was segmented on the basis of Brodmann areas 9 and 10. The sensorimotor cortex on Brodmann areas 1, 2, 3 and 4¹². To calculate the average ADC and FA of the five white matter pathways FibreTrak was used (release 2.5.3, Philips Medical Systems, Best, The Netherlands). The software applies fiber assignment by continuous tracking²⁵. The following standard parameters were implemented: minimum FA value 0.10, maximum angle change 27°, minimum fiber length 10 mm. For more detailed information on the application of the fiber tracking software see the supplementary material.

Clinical Assessments

From the extensive assessment battery in the TRACK-HD study, specific tasks were chosen that gave a representation of functioning in each symptom domain. Furthermore, these were tasks that had been proved to provide sensitive outcome measures for group comparisons, even in the premanifest stages⁴: index finger speeded tapping and sustained tongue force measures (motor), anti-saccade latency and error rate (oculomotor), symbol digit modalities test, the Stroop word reading test, trail making task part B, and a visual working memory task – the spot the change task (cognition); Beck's depression inventory 2nd version (BDI-II) and the frontal systems behavior inventory which yields three subscores of disinhibition, executive functioning and apathy (psychiatry). CAG repeat length and probability of onset within 5 years and Burden of pathology $((\text{CAG} - 35.5) \times \text{age})^{26}$ were also added to the analysis. For the complete set of clinical assessments and variables see Tabrizi *et al.* (2009)⁴.

Statistics

Statistical analyses were performed with the Statistical Package for Social Sciences (SPSS for Windows; version 17.0.2, SPSS inc, Chicago, IL). Distributions and assumptions were checked. Independent student's t-tests and Chi-square tests were applied where appropriate in the analysis of group differences based on descriptive data; age, CAG, Dutch adult reading test (IQ), TFC and UHDRS. To test for differences in FA and ADC in the three ROIs and the five white matter fiber bundles between premanifest or manifest gene carriers and their corresponding control groups, analyses were performed using independent student's t-tests. Correction for multiple comparisons was applied to each analysis. Each analysis of ADC in the basal ganglia ROIs, the FA in the basal ganglia ROIs, the FA of the fiber pathways, and the ADC of the fiber pathways was regarded as a separate analyses. Therefore a Bonferroni correction was applied to each analysis. For the ADC and FA ROI analysis this lead to $0.05/3 = 0.017$, and for the ADC and FA fiber pathways analysis this lead this to $0.05/5 = 0.01$. The number of voxels in each seed ROI was compared between groups. Partial Pearson correlations analysis was performed to explore and test for possible associations between measures of white matter fiber pathway integrity and clinical measures. Age and gender were added into this analysis as covariates. The number of voxels in a ROI were also correlated to the clinical variables in order to examine the possibility that grey matter volume explains any possible correlations. The ADC and FA values of the white matter fiber pathways were correlated to each other to examine other explanations for possible results.

Results

Premanifest

No differences in age, gender, IQ, TFC, and UHDRS motor score between the premanifest gene carriers and their controls were present (Table I). The ADC and FA values of the ROIs and fiber pathways are shown in Table I. Premanifest gene carriers showed increased ADC values in the corpus callosum compared with controls. A significant increase in ADC of the white matter fibers of the sensorimotor cortex was also found between premanifest gene carriers and controls. No differences in ADC were found in the regions of the caudate nucleus and thalamus. No difference in FA was found in any of the three regions between the two groups. Also, no FA or ADC differences were found in any of the fiber pathways between the two groups. The number of voxels in the caudate nucleus ROI of premanifest group is significantly lower than the number in the control group ROI.

Early HD

The demographic data of the early HD and control group B showed no differences in age, gender or IQ. TFC and UHDRS differed significantly (Table II). In the corpus callosum and the caudate nucleus, the ADC values were larger in early HD when compared with controls. Between the two groups, no difference in FA was found in any of the ROIs. ADC values were significantly increased in fibers from all regions, except for the caudate nucleus fibers. FA was decreased in fibers running to and from the prefrontal cortex in early HD patients. No difference in FA was found in fibers passing through the corpus callosum, caudate nucleus, thalamus and sensorimotor cortex. The number of voxels of the caudate nucleus as well as in the corpus callosum was significantly lower in the patient group than in the control group (Table II).

Clinical correlations

The correlation analysis between the ADC of the fiber bundles with genetics, probability of onset within five years, burden of pathology, motor, oculomotor, cognition and behavior in all participants are shown in Table III.

Tapping was moderately associated with the diffusivity (ADC) of bundles through the corpus callosum, thalamus, sensorimotor cortex and prefrontal cortex. For the tongue force, similar but weaker associations were found. Latency of anti-saccades and the percentage of antisaccade errors in the oculomotor task were found to correlate with increased diffusivity of the corpus callosum, sensorimotor cortex and prefrontal cortex fibers. All cognitive measures were moderately to strongly associated with the ADC of fibers through the corpus callosum, sensorimotor cortex

and to a lesser extent the prefrontal cortex. In premanifest gene carriers, probability of expected onset within 5 years and burden of pathology showed a high positive correlation with the diffusivity of the corpus callosum fibers and with those of the sensorimotor cortex, whereby a loss of integrity related to a higher probability of onset within five years and higher burden of pathology. No association in any cognitive domain with fibers of the thalamus was found. CAG repeat length and behavioral measures did not show association with the ADC of any of the fiber bundles studied. No measures showed association with the fibers of the caudate nucleus. FA of the corpus callosum and sensorimotor cortex fibers negatively correlated with the latency ($r = -0.52$, $p < 0.001$) and percentage of errors ($r = -.038$, $p = 0.001$) in the anti-saccade oculomotor task. FA did not demonstrate any significant correlation with genetics, motor, cognition, and behavior.

The results from a correlational analysis between number of voxels in a seed region and clinical variables showed five significant moderate correlations. Only one of these also showed a significant correlation in the analysis of ADC values with clinical variables. This was the correlation between the caudate nucleus and TMT task performance ($r = -0.36$, $p < 0.01$). Directly correlating the ADC and FA values of the white matter pathways with each other revealed a number of significant correlations which is shown in table IV in the supplementary material. The direct correlation of ADC and FA of the same fiber bundle shows that the ADC and FA of the sensorimotor cortex and prefrontal white matter pathways are correlated.

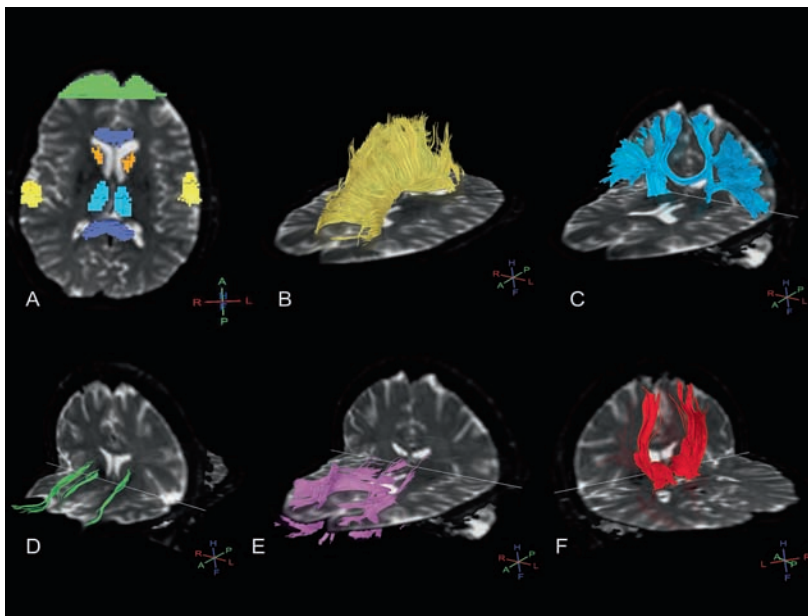


Figure 1. Typical example of ROIs (A) and subsequent white matter fiber pathways in a premanifest gene carrier of the corpus callosum (B), sensorimotor cortex (C), caudate nucleus (D), prefrontal cortex (E) and thalamus (F). 3D crosses depict orientation, whereby H = head, F = feet, A = anterior, P = posterior, R = right, L = left.

Table 1. Group demographics, ADC and FA values, and number of seed voxels per region of interest for the premanifest gene carriers and their controls.

	Control group A n: 14, male: 7		Premanifest gene carriers n: 27, male: 16		
	Mean (SD)	range	Mean (SD)	range	
Age (yrs)	46 (7,5)	35 - 58	43 (8,3)	26 - 61	
CAG	- (-)	-	43 (2,5)	39 - 50	
IQ	105,6 (11,3)	88 - 130	101,3 (11,3)	76 - 118	
TFC	13 (0)	13 - 13	12,6 (0,8)	10 - 13	
UHDRS	1,9 (1,8)	0 - 6	2,4 (1,4)	0 - 4	
ADC ROI	# voxels ± SD	mean ± SD	# voxels ± SD	mean ± SD	<i>p</i>
Corpus Callosum	1884 ± 378	0.78 ± 0.028	1767 ± 319	0.81 ± 0.033*	0.014
Caudate Nucleus	58 ± 13	0.73 ± 0.071	47 ± 11***	0.76 ± 0.053	0.160
Thalamus	2700 ± 843	0.73 ± 0.023	2601 ± 657	0.73 ± 0.023	0.994
FA ROI					
Corpus Callosum	1884 ± 378	0.76 ± 0.019	1767 ± 319	0.75 ± 0.021	0.461
Caudate Nucleus	58 ± 13	0.17 ± 0.015	47 ± 11***	0.18 ± 0.023	0.058
Thalamus	2700 ± 843	0.34 ± 0.025	2601 ± 657	0.33 ± 0.022	0.368
ADC Fiber pathway	# voxels ± SD	mean ± SD	# voxels ± SD	mean ± SD	
Corpus Callosum	1884 ± 378	0.89 ± 0.049	1767 ± 319	0.91 ± 0.054	0.206
Caudate Nucleus	58 ± 13	0.98 ± 0.116	47 ± 11***	0.94 ± 0.075	0.166
Thalamus	2700 ± 843	0.87 ± 0.055	2601 ± 657	0.89 ± 0.071	0.476
Motor cortex	595 ± 86	0.78 ± 0.017	580 ± 71	0.80 ± 0.029**	0.009
Prefrontal cortex	1136 ± 183	0.88 ± 0.044	1117 ± 322	0.89 ± 0.037	0.631
FA Fiber pathway					
Corpus Callosum	1884 ± 378	0.49 ± 0.015	1767 ± 319	0.49 ± 0.016	0.785
Caudate Nucleus	58 ± 13	0.36 ± 0.017	47 ± 11***	0.35 ± 0.031	0.683
Thalamus	2700 ± 843	0.42 ± 0.018	2601 ± 657	0.41 ± 0.021	0.515
Motor cortex	595 ± 86	0.40 ± 0.017	580 ± 71	0.39 ± 0.020	0.190
Prefrontal cortex	1136 ± 183	0.41 ± 0.018	1117 ± 322	0.40 ± 0.021	0.120

SD: standard deviation, CAG: CAG repeat length, IQ: estimate of premorbid intelligence quotient. TFC: Total Functional Capacity score. UHDRS: Unified Huntington's Disease Rating Scale total motor score. ROI: Region of interest analysis. ADC: Apparent Diffusion Coefficient in $\mu\text{m}^2/\text{ms}$, FA: Fractional Anisotropy (no unit), Fiber pathway: fiber pathways analysis between the listed region and the rest of the brain. * $p < 0.017$, ** $p < 0.01$ (adjusted for multiple comparisons). # voxels: mean number of voxels in the listed seed region. ***Number of voxels differs significantly from healthy controls

Table 2. Group demographics, ADC and FA values, and number of seed voxels per region of interest for the early HD patients and their controls.

	Control group B n: 14, male: 7		Early HD n: 16, male: 12		<i>p</i>
	Mean (SD)	range	Mean (SD)	range	
Age (yrs)	51.4 (7.9)	42 - 65	48.2 (10)	31 - 63	
CAG	- (-)	-	43 (1.6)	41 - 46	
IQ	102.6 (6.6)	88 - 115	99.6 (12)	72 - 118	
TFC	12.9 (0.3)	12 - 13	10.6 [§] (2)	7 - 13	
UHDRS	3.1 (2.8)	0 - 7	18.3 [§] (10.4)	6 - 45	
ADC ROI	# voxels ± SD	mean ± SD	# voxels ± SD	mean ± SD	<i>p</i>
Corpus Callosum	1934 ± 312	0.80 ± 0.031	1445 ± 371***	0.85 ± 0.040*	0.000
Caudate Nucleus	57 ± 12	0.74 ± 0.048	40 ± 7***	0.83 ± 0.069*	0.001
Thalamus	2480 ± 531	0.74 ± 0.032	3102 ± 1062	0.74 ± 0.034	0.863
FA ROI					
Corpus Callosum	1934 ± 312	0.75 ± 0.012	1445 ± 371***	0.73 ± 0.033	0.046
Caudate Nucleus	57 ± 12	0.17 ± 0.018	40 ± 7***	0.19 ± 0.019	0.072
Thalamus	2480 ± 531	0.33 ± 0.021	3102 ± 1062	0.32 ± 0.034	0.95
ADC Fiber pathway	# voxels ± SD	mean ± SD	# voxels ± SD	mean ± SD	
Corpus Callosum	1934 ± 312	0.89 ± 0.051	1445 ± 371***	0.95 ± 0.067**	0.008
Caudate Nucleus	57 ± 12	0.88 ± 0.107	40 ± 7***	0.97 ± 0.079	0.023
Thalamus	2480 ± 531	0.85 ± 0.080	3102 ± 1062	0.93 ± 0.063**	0.007
Motor cortex	589 ± 117	0.79 ± 0.023	593 ± 110	0.82 ± 0.027**	0.001
Prefrontal cortex	1118 ± 239	0.88 ± 0.023	1202 ± 274	0.95 ± 0.056**	0.000
FA Fiber pathway					
Corpus Callosum	1934 ± 312	0.48 ± 0.013	1445 ± 371***	0.47 ± 0.017	0.027
Caudate Nucleus	57 ± 12	0.35 ± 0.027	40 ± 7***	0.35 ± 0.021	0.592
Thalamus	2480 ± 531	0.41 ± 0.016	3102 ± 1062	0.41 ± 0.024	0.644
Motor cortex	589 ± 117	0.38 ± 0.019	593 ± 110	0.37 ± 0.024	0.059
Prefrontal cortex	1118 ± 239	0.39 ± 0.016	1202 ± 274	0.38 ± 0.014**	0.006

SD: standard deviation, CAG: CAG repeat length, IQ: estimate of premorbid intelligence quotient. TFC: Total Functional Capacity score. UHDRS: Unified Huntington's Disease Rating Scale total motor score.

[§]Significant difference from control group, *p* < 0.01. ROI: Region of interest analysis. ADC: Apparent Diffusion Coefficient in $\mu\text{m}^2/\text{ms}$, FA: Fractional Anisotropy (no unit), Fiber pathway: fiber pathways analysis between the listed region and the rest of the brain. **p* < 0.017, ***p* < 0.01 (adjusted for multiple comparisons). # voxels: mean number of voxels in the listed seed region. ***Number of voxels differs significantly from healthy controls.

Table 3. Standardized correlation coefficients matrix for ADC of white matter fiber bundles and clinical measures in all participants.

	Motor			Cognitive				Behavior			
	Tapping	Tongue	SDMT	SWR	TMT B	SPOT	BDI-II	FrSBe Dis-inhib	FrSBe Exec dysf	FrSBe apathy	
Corpus Callosum	0.38**	0.27	-0.32*	-0.39**	0.36**	-0.39**	0.11	0.01	0.09	0.10	
Caudate Nucleus	0.13	0.23	-0.08	-0.04	0.13	-0.19	-0.05	0.05	-0.02	-0.01	
Thalamus	0.41**	0.33*	-0.27	-0.28	0.26	-0.30	0.02	0.03	0.09	0.07	
Motor cortex	0.46**	0.32*	-0.46**	-0.52**	0.55**	-0.33*	0.15	-0.02	0.11	0.17	
Prefrontal cortex	0.33*	0.28	-0.28	-0.34*	0.25	-0.28	0.15	-0.02	-0.06	0.04	
	Genetics	Probability of onset	Burden of Pathology				Oculomotor				
	CAG	Gene carrier only	within 5 years (preHD only)	(CAG-35.5) x age	Latency of anti-saccades	Error % of anti-saccades					
Corpus Callosum	0.36		0.61**	0.51**	-0.32*	-0.39**					
Caudate Nucleus	0.09		0.42	0.27	-0.08	-0.04					
Thalamus	0.10		0.06	0.19	-0.27	-0.28					
Motor cortex	0.32		0.58**	0.52**	-0.46**	-0.52**					
Prefrontal cortex	0.09		0.41*	0.37	-0.28	-0.34*					

Tapping = Average speeded tapping intertap variability for left and right index finger, Tongue = sustained tongue force measure, SDMT = Symbol Digit Modalities test, SWR = Stroop word reading task, TMT B = Trail making test part B, SPOT = Visual array comparison task for visual short-term memory capacity, BDI-II = Beck's Depression Inventory 2nd version, FrSBe = Frontal Systems Behaviour rating scale Self Report, disinhibition, executive dysfunction and apathy subscores, CAG = CAG repeat length (in gene carriers only), Expected years to onset correlations are only for premanifest gene carriers. All correlations are controlled for the effects of age and gender. * $p < 0.01$ ** $p < 0.005$

Discussion

The main finding of this study is that in premanifest gene carriers, the white matter pathway of the sensorimotor cortex is impaired. Furthermore, our data show that in the early manifest phase of the disease impairment is more widespread and present in the white matter pathways of the sensorimotor cortex, corpus callosum, thalamus, and prefrontal cortex. Finally, a relationship is seen between the changes in white matter pathways and functionality in the domains of motor, oculomotor and cognition. Moreover this study confirms findings of regional differences in the corpus callosum of premanifest and the caudate nuclei and corpus callosum of early HD^{14,27}.

In the premanifest phase of the disease, our study demonstrated a reduction of integrity of only the sensorimotor cortex fibers pathway, therefore this suggests that this pathway may be one of the first to be affected by HD. This is supported by the positive relationship between a higher probability of onset within 5 years, and a higher burden of pathology, with the loss of integrity of the sensorimotor cortex fibers. This premanifest cohort is 'free' of motor symptoms, and therefore these findings in a truly 'premotor' premanifest group further support the idea that these white matter changes are among the first to occur. This study is the first to demonstrate this change across the whole pathway; however, other studies examining this area do provide support for this finding. The findings of the voxel-by-voxel white matter analysis of Reading *et al.* (2005)¹² found differences in a cluster of voxels coinciding with the primary motor cortex (Brodmann area 4). Atrophy of the sensorimotor cortex was demonstrated as the only cortical region to be affected in premanifest gene carriers far from predicted onset⁴. Furthermore differences have been reported in functions that utilize this area in premanifest gene carriers, such as measures of motor function^{5,28}. The other important finding of our study in premanifest gene carriers is the differences in diffusivity in the corpus callosum, thereby replicating previous findings by Rosas *et al.* (2006,2009)^{14,27}. However we add that these differences are not seen in the white matter projections specifically going to and from the corpus callosum. Therefore, when looking beyond the main structure it can be suggested that the loss of integrity of the main structure is apparent, but not spread over its entire network, as is the case in manifest HD.

In the early manifest phase of HD, our data show that the diffusivity of the fiber pathways of the thalamus, corpus callosum, sensorimotor, and prefrontal cortex was higher in HD than in healthy controls. This suggests a disintegration of these structures. Of the five white matter pathways examined in HD all were found to be

affected except the pathways of the caudate nuclei. The absence of affected white matter from the caudate nucleus should be interpreted with some caution. It may suggest that the magnitude of integrity loss may not be the same for a structure as for its fibers at a given stage of the disease. However the variance of these measurements is larger than that of the other fibers pathways. The remaining results, such as that of reduced integrity of the prefrontal cortex fibers, find support in the regional differences demonstrated by Rosas *et al.* (2006)¹⁴. Our results show changes in ADC and almost no changes in FA. This suggests that of these two closely related measures, ADC is more sensitive in demonstrating changes across large pathways in HD. The results of the regional analysis showed higher diffusivity in the caudate nucleus and corpus callosum in HD than in healthy controls. This was not the case in the thalamus, whereby similar diffusion properties were seen in both HD and controls. Our findings concur with previous cross-sectional and longitudinal findings of a widespread effect of HD on white matter^{14;20;22;29}. The finding that a region was not affected, but its fibers were, demonstrates the need to embrace the full potential of DTI measures for HD, as this shows that despite a structure not showing integrity differences, the fibers that are needed for this structure to communicate with the brain may well be affected. In the case of the thalamus this is especially relevant to the clinical expression of the disease as this structure is vital to a large number of functional processes.

The previously discussed outcomes demonstrate that almost all fiber pathways that we examined are affected in early manifest HD and that one specific pathway is also affected in premanifest gene carriers. In exploring the clinical implications of these findings we see strong relationships between both motor, oculomotor and cognitive measures, and diffusivity measures of the pathways of the corpus callosum, thalamus, sensorimotor and prefrontal cortex. Although one cognitive measure does correlate to the prefrontal cortex fiber the cognitive measures are most strongly related to the sensorimotor cortex fibers. This finding can be explained with two complementary hypotheses. First, as seen in the premanifest group, the fibers of the sensorimotor cortex are the first to show decreased integrity. This suggests that these are the most severely affected fibers in the earliest (premanifest) stages of HD; therefore, it is not surprising that the clinical measures of decline relate to these fibers. Second, HD effects both cognition and motor function, and all cognitive tests require a motor response. A consequent finding in cognitive HD literature is that cognitive tests sensitive to psychomotor speed are the most sensitive tasks. A great deal of voluntary motor functioning is initiated in the sensorimotor cortex. Because of this we were not entirely surprised that cognitive tests relate strongly to the fibers of the sensorimotor cortex. The tasks chosen for analysis were those that provide meaningful outcomes for all

study groups, and did not show ceiling or floor effects. Therefore, we can conclude that fibers associated with higher order cognitive and motor coordination are affected in a manner that is congruent to clinical manifestations and that for this reason, DTI measures can be applied to characterize the structure-function relationship of white matter. This conclusion is supported in other studies of white and grey matter and clinical measures^{6,30}. In another study of eye movements and fiber tracking, similar results were found as ours, especially finding a relationship between eye movements and fiber FA³¹. We did not show a relationship between CAG repeat length or behavioral processes and changes in white matter integrity. The CAG repeat length is not dependent on disease progression or white matter pathways and this stable quality may, in part, explain this finding. A possible explanation for the absence of a relationship between behavioral measures and diffusivity may be the complex pathophysiological and psychological process underlying these behavioral changes that may not be primarily dependent on white matter. Alternatively, the use of medication may be a factor in the level of symptoms reported (full details of medication use are outlined in Tabrizi *et al.* (2009)⁴ leading to an underestimation of neuropsychiatric problem behavior. However, a recent study has shown that behavioral changes in premanifest HD remain stable³², thereby reinforcing the idea that degenerative processes are not at the root of these neuropsychiatric differences. Therefore we conclude that behavioral changes may not be directly reflected by white matter changes.

This study examined and demonstrated differences in white matter pathways of five HD relevant regions, this restriction is a limitation of the study. Differences were found in the number of seed voxels in the caudate nucleus in premanifest gene carriers and in the caudate nucleus and corpus callosum in manifest HD. On the contrary, differences were not seen in the number of voxels in the thalamus, sensorimotor region, or prefrontal regions in the patient group. These reductions do seem to reflect expected atrophy, but do not follow the pattern of differences found in ADC. Therefore these differences do not seem to explain the differences in diffusivity. The results from a correlation analysis between number of voxels in a seed region and clinical variables reveal only five significant moderate correlations. This is in contrast to the analysis of relationship between average ADC and the clinical variables whereby 25 moderate to high correlations were significant. Furthermore only one of these five was the same as one of the 25 clinical correlations. These results suggest the volume of the seed region does not explain the observed original correlations. With this possibility excluded, it can be stated with more certainty that the relationships observed reflect the underlying changes in structure of the white matter pathways. Furthermore, direct correlation of the ADC and FA of the white matter pathways also supports this conclusion.

It can be seen that only significant relationships between the ADC and FA of the same pathways were apparent for pathways that showed (nearly) significant group differences. Overall, the results call for further examination of white matter pathways. The findings warrant confirmation with longitudinal follow-up.

In conclusion, we demonstrated that the sensorimotor cortex fibers are affected already in the premanifest phase of HD and therefore may be a good target for following progression of the disease. Our data show that impairment is seen in corpus callosum, nuclei and fiber projections of HD relevant brain regions in both premanifest and early manifest HD. These impairments relate to proven correlates of clinical dysfunction. Overall, the findings of this study confirm the feasibility and use of DTI measures in HD research, whereby we show that ADC is a good measure in characterizing the impaired function-structure relationship present in HD.

Acknowledgments

The authors wish to thank the TRACK-HD study participants, the “CHDI/High Q Foundation”, a not-for-profit organization dedicated to finding treatments for HD, for providing financial support (www.chdifoundation.org), and all TRACK-HD investigators for their efforts in conducting this study (www.track-hd.net). We would like to thank BioRep for the CAG determinations. We would also like to acknowledge the following individuals personally for their contributions. Caroline Jurgens, Marie-Noelle Witjes-Ane and Ellen 't Hart for assistance with coordination and data collection, Gail Owen for coordination of data transfer, Mike Sharman for his comments and input and Felix Mudoh Tita for data monitoring.

References

1. Roos RA, Bots GT, Hermans J. Quantitative analysis of morphological features in Huntington's disease. *Acta Neurol Scand* 1986;73:131-35
2. Aylward EH, Li Q, Stine OC, et al. Longitudinal change in basal ganglia volume in patients with Huntington's disease. *Neurology* 1997;48:394-99
3. Rosas HD, Liu AK, Hersch S, et al. Regional and progressive thinning of the cortical ribbon in Huntington's disease. *Neurology* 2002;58:695-701
4. Tabrizi SJ, Langbehn DR, Leavitt BR, et al. Biological and clinical manifestations of Huntington's disease in the longitudinal TRACK-HD study: cross-sectional analysis of baseline data. *Lancet Neurol* 2009;8:791-801
5. Paulsen JS, Langbehn DR, Stout JC, et al. Detection of Huntington's disease decades before diagnosis: the Predict-HD study. *J Neurol Neurosurg Psychiatry* 2008;79:874-80
6. Beglinger LJ, Nopoulos PC, Jorge RE, et al. White matter volume and cognitive dysfunction in early Huntington's disease. *Cogn Behav Neurol* 2005;18:102-07
7. Fennema-Notestine C, Archibald SL, Jacobson MW, et al. In vivo evidence of cerebellar atrophy and cerebral white matter loss in Huntington disease. *Neurology* 2004;63:989-95
8. Aylward EH, Anderson NB, Bylsma FW, et al. Frontal lobe volume in patients with Huntington's disease. *Neurology* 1998;50:252-58
9. Jech R, Klempir J, Vymazal J, et al. Variation of selective gray and white matter atrophy in Huntington's disease. *Mov Disord* 2007;22:1783-89
10. Paulsen JS, Hayden M, Stout JC, et al. Preparing for preventive clinical trials: the Predict-HD study. *Arch Neurol* 2006;63:883-90
11. Nucifora PG, Verma R, Lee SK, et al. Diffusion-tensor MR imaging and tractography: exploring brain microstructure and connectivity. *Radiology* 2007;245:367-84
12. Reading SA, Yassa MA, Bakker A, et al. Regional white matter change in pre-symptomatic Huntington's disease: a diffusion tensor imaging study. *Psychiatry Res* 2005;140:55-62
13. Magnotta VA, Kim J, Kosciak T, et al. Diffusion Tensor Imaging in Preclinical Huntington's Disease. *Brain Imaging and Behavior* 2009;3:77-84
14. Rosas HD, Tuch DS, Hevelone ND, et al. Diffusion tensor imaging in presymptomatic and early Huntington's disease: Selective white matter pathology and its relationship to clinical measures. *Mov Disord* 2006;21:1317-25
15. Mori S, van Zijl PC. Fiber tracking: principles and strategies - a technical review. *NMR Biomed* 2002;15:468-80
16. Stebbins GT, Murphy CM. Diffusion tensor imaging in Alzheimer's disease and mild cognitive impairment. *Behav Neurol* 2009;21:39-49
17. Rizzo G, Martinelli P, Manners D, et al. Diffusion-weighted brain imaging study of patients with clinical diagnosis of corticobasal degeneration, progressive supranuclear palsy and Parkinson's disease. *Brain* 2008;131:2690-700
18. Zhang K, Yu C, Zhang Y, et al. Voxel-based analysis of diffusion tensor indices in the brain in patients with Parkinson's disease. *Eur J Radiol*. 2011 Feb;77(2):269-73.
19. Mascalchi M, Lolli F, Della NR, et al. Huntington disease: volumetric, diffusion-weighted, and magnetization transfer MR imaging of brain. *Radiology* 2004;232:867-73
20. Vandenberghe W, Demaerel P, Dom R, et al. Diffusion-weighted versus volumetric imaging of the striatum in early symptomatic Huntington disease. *Journal of Neurology* 2009;256:109-14
21. Sritharan A, Egan G, Johnston L, et al. A longitudinal diffusion tensor imaging study in symptomatic Huntington's disease. *J Neurol Neurosurg Psychiatry*. 2010 Mar;81(3):257-62.
22. Douaud G, Behrens TE, Poupon C, et al. In vivo evidence for the selective subcortical degeneration in Huntington's disease. *Neuroimage* 2009;46:958-66
23. Stout JC, Weaver M, Solomon AC, et al. Are cognitive changes progressive in prediagnostic HD? *Cogn Behav Neurol* 2007;20:212-18

24. Lasker AG, Zee DS. Ocular motor abnormalities in Huntington's disease. *Vision Res* 1997;37(24):3639-45
25. Mori S, Crain BJ, Chacko VP, et al. Three-dimensional tracking of axonal projections in the brain by magnetic resonance imaging. *Ann Neurol* 1999;45:265-69
26. Penney JB, Vonsattel JP, MacDonald ME, et al. CAG repeat number governs the development rate of pathology in Huntington's disease. *Annals of Neurology* 1997;41:689-92
27. Rosas HD, Lee SY, Bender A, et al. Altered white matter microstructure in the corpus callosum in Huntington's disease: Implications for cortical "disconnection". *Neuroimage*. 2010 Feb 15;49(4):2995-3004.
28. Solomon AC, Stout JC, Weaver M, et al. Ten-year rate of longitudinal change in neurocognitive and motor function in prediagnosis Huntington disease. *Mov Disord* 2008;23:1830-36
29. Weaver KE, Richards TL, Liang O, et al. Longitudinal diffusion tensor imaging in Huntington's Disease. *Exp Neurol* 2009;216:525-29
30. Wolf RC, Vasic N, Schonfeldt-Lecuona C, et al. Cortical dysfunction in patients with Huntington's disease during working memory performance. *Hum Brain Mapp*. 2009 Jan;30(1):327-39.
31. Kloppel S, Draganski B, Golding CV, et al. White matter connections reflect changes in voluntary-guided saccades in pre-symptomatic Huntington's disease. *Brain* 2008;131:196-204
32. van Duijn E, Kingma EM, Timman R, et al. Cross-sectional study on prevalences of psychiatric disorders in mutation carriers of Huntington's disease compared with mutation-negative first-degree relatives. *J Clin Psychiatry* 2008;69:1804-10

Supplementary Material

Supplementary Methods

Segmentation

Based on the anatomical co-registration images, the ROIs were segmented in native space for each individual. This was done by two experienced radiographers, blinded to patient group. Two types of ROIs were defined. Basal ganglia ROIs for analysis, and seed-ROIs as starting point for fiber tracking. The basal ganglia ROIs were segmented as follows. For the caudate nucleus all voxels clearly bounded by the lateral ventricle and the anterior limb of the internal capsule were selected. The putamen segmentation included all voxels within the structure bounded on the medial side by the globus pallidus and the anterior limb of the internal capsule, and on the lateral side by the capsula extrema. The thalamus segmentation was performed by allocating all voxels to the ROI that medially bordered the third ventricle, were superiorly bordered by the lateral ventricle, and were laterally bordered by the internal capsule. The seed ROIs were cortically based, and because these areas were not as clearly anatomically bounded as the other structures, Brodmann areas were used to define the segmentation. Reading *et al.* (2005) defined areas of the cortex in their analysis of presymptomatic HD by means of these Brodmann areas¹. The superior prefrontal region was segmented on areas 9 (frontal portion) and 10. Brodmann area 10 is medially bound by the superior rostral sulcus, and dorsally by the inferior frontal sulcus and the frontomarginal sulcus. Area 9 bordered inferiorly by area 10 and dorsally by the superior frontal sulcus. After all ROIs were drawn, the radiographers switched scans and carefully checked the segmentations for potential miss-segmentation. After all scans had been segmented a random 20% were selected for verification by a neurologist specialized in neuro-imaging. Any segmentation voxels that were felt to be outside of the targeted anatomy were discussed until a consensus was formed and these few voxels were changed accordingly.

Analysis

We applied the software supplied by the manufacturer by transferring the raw DTI data and the anatomic co-registration images to an off-line manufacturer provided console. In doing so the data were loaded into the Philips Research Image-processing Development Environment (PRIDE) (Philips Medical Systems). Then the diffusion tensor and derived measures, including ADC and FA, were calculated using the Philips PRIDE Fiber Tracking tool (version 2.5.3). This allows fiber tracking based on the Fiber Assignment by Continuous Tracking (FACT) algorithm². The algorithm values for restricting fiber tracking were kept at default

Supplementary Results

Table 4. Cross tabulation of correlation coefficients of the FA and ADC of the white matter fiber pathways with each other.

		Corpus Callosum		Caudate Nucleus		Thalamus		Motor cortex		Prefrontal cortex	
		ADC	FA	ADC	FA	ADC	FA	ADC	FA	ADC	FA
Corpus Callosum	ADC	-	-.123	.482	-.262	.705	.069	.644	-.312	.572	-.432
	FA		-	.002	.136	-.065	.472	-.439	.581	-.272	.516
Caudate Nucleus	ADC			-	.028	.594	.153	.185	.091	.206	-.077
	FA				-	-.116	.404	-.052	.190	-.352	.046
Thalamus	ADC					-	.034	.476	-.145	.353	-.183
	FA						-	-.021	.290	-.050	.126
Motor cortex	ADC							-	-.604	.548	-.530
	FA								-	-.492	.473
Prefrontal cortex	ADC									-	-.483
	FA										-

ADC: Apparent Diffusion Coefficient, FA: Fractional Anisotropy. **Bold** = significant correlation

and were: minimum FA value of 0.10, maximum angle change: 27°, and a minimum fiber length of 10mm. This same method and software has been applied in a number of disorders of both brain and muscle, such as developmental CNS anomalies³, corticospinal tract stroke⁴, lateral patellar dislocation⁵ and Lissencephaly⁶.

References

1. Reading SA, Yassa MA, Bakker A, et al. Regional white matter change in pre-symptomatic Huntington's disease: a diffusion tensor imaging study. *Psychiatry Res* 2005;140:55-62
2. Mori S, Crain BJ, Chacko VP, et al. Three-dimensional tracking of axonal projections in the brain by magnetic resonance imaging. *Ann Neurol* 1999;45(2):265-69
3. Lee SK, Kim DI, Kim J, et al. Diffusion-tensor MR imaging and fiber tractography: a new method of describing aberrant fiber connections in developmental CNS anomalies. *Radiographics* 2005;25:53-65
4. Lee JS, Han MK, Kim SH, et al. Fiber tracking by diffusion tensor imaging in corticospinal tract stroke: Topographical correlation with clinical symptoms. *Neuroimage* 2005;26:771-76
5. Kan JH, Heemskerk AM, Ding Z, et al. DTI-based muscle fiber tracking of the quadriceps mechanism in lateral patellar dislocation. *J Magn Reson Imaging* 2009;29:663-70
6. Rollins, N., Reyes, T., Chia, J., 2005. Diffusion tensor imaging in lissencephaly. *AJNR Am.J.Neuroradiol.* 26, 1583-1586.